e-ISSN: 2689-4934

Available online at
http://uppp.uitm.edu.my/online-issues.html

ESTEEM Academic Journal Vol 20, September 2024, 25-39

ESTEEM **Academic Journal (EAJ)**

Magnetic graphene oxide incorporated with Fe_2O_3 for the removal of lead (II) ions

Norhusna Mohamad Nor[1,2*], Nur Alwani Ali Bashah[1], Nor Syazwani Mohamed Noor[1], Nur Afifah Atikah Yaakob[1]

[1]*Chemical Engineering Studies, College of Engineering, Universiti Teknologi MARA, Cawangan Pulau Pinang, 13500 Permatang Pauh, Pulau Pinang, Malaysia*

[2]*Waste Management and Resource Recovery (WeResCue) Group, Chemical Engineering Studies, College of Engineering, Universiti Teknologi MARA, Cawangan Pulau Pinang, 13500 Permatang Pauh, Pulau Pinang, Malaysia*

ARTICLE INFO

Article history:
Received 1 March 2024
Revised 1 August 2024
Accepted 21 August 2024
Online first
Published 25 September 2024

Keywords:
Adsorption
Fe_2O_3 impregnation
Graphene oxide
Pb^{2+} removal
Wastewater
Isotherms

DOI:
10.24191/esteem.v20iSeptember.2924.g1578

ABSTRACT

The objective of this research work is to synthesise graphene oxide (GO) with iron oxide (Fe_2O_3) nanoparticles as a magnetic adsorbent for lead ion (Pb^{2+}) removal. In this work, the effect of synthesis parameters of GO/Fe_2O_3 (Fe_2O_3 loading weight ratio, synthesis time and calcination temperature) and adsorption parameters (initial Pb^{2+} concentration, adsorption temperature and contact time) on Pb^{2+} removal were investigated. The adsorption experiment was carried out in a batch system, and the synthesised GO/Fe_2O_3 adsorbent was characterised using TGA and N_2 sorption-desorption analyses. The adsorption characteristics of Pb^{2+} using GO/Fe_2O_3 adsorbent were analysed using adsorption isotherms and kinetic study. The optimal synthesis parameters were found to be a 1:0.5 ratio for GO/Fe_2O_3, a synthesis time of 60 min and a calcination temperature of 400°C, resulting in a Pb^{2+} removal rate of 96% and adsorption capacity of 49.85 mg Pb^{2+}/g adsorbent. The GO/Fe_2O_3 adsorbent synthesised at 400°C and a 1:0.5 ratio exhibits a larger surface area and smaller pore diameter, 98.20 m^2/g and 15.67 nm, respectively, compared to other samples. Increasing the synthesis temperature decreases the growth and formation of GO/Fe_2O_3, reducing the surface area. Experimental results revealed that the adsorption of Pb^{2+} using GO/Fe_2O_3 adsorbent fitted the pseudo-second-order kinetic and was best described by the Langmuir isotherm with a high correlation coefficient (R^2 >0.99).

[1*] Corresponding author. *E-mail address: norhusna8711@uitm.edu.my*

https://doi.org/10.24191/esteem.v20iSeptember.2924.g1578

1. INTRODUCTION

Malaysia is one of the developing countries facing environmental pollution problems due to economic growth driven by various industries. Although many benefited economically this has resulted in the production of high volumes of pollutants. Water contamination has been a critical challenge, affecting agriculture, the environment, and human survival. The presence of heavy metals in water has received the public's attention since they pose a threat to human health and ecosystems. Due to the discharge of heavy metals from industrial activities, water quality in some of Malaysia's rivers has severely decreased [1]. Among other available heavy metal pollutants, this research will focus on the adsorptive characteristics of one targeted pollutant: lead ion (Pb^{2+}). In general, Pb^{2+} exists in rivers across the world due to industrial activities such as the combustion of fossil fuels, the mining industry, the production of lead-acid batteries, semiconductors, electroplating and other metal-related industries [2].

According to the Department of Environment (DOE) Malaysia's regulation (Environmental Quality Act, 1974), the permissible concentrations of Pb^{2+} to be discharged into rivers for Standard A and B are 0.10 and 0.50 mg/L, respectively [3]. Significant health issues include kidney damage, liver damage, high blood pressure, and brain and central nervous system damage, which will all be adversely affected by excessive Pb^{2+} exposure. Additionally, short exposure to Pb^{2+} poisoning might result in anaemia, vomiting, and abdominal pain [4]. To fulfil the DOE minimal requirement, various removal technologies to mitigate the presence of Pb^{2+} in rivers have been developed and applied in industries, such as coagulation-flocculation, chemical precipitation, electrochemical treatment, ion exchange, membrane separation, and adsorption [5]. Among these technologies, adsorption is the most affordable, efficient, and commercially viable [6]. For the removal of Pb^{2+}, a variety of adsorbents have been utilised, such as biomass, activated carbon, clay minerals (such as kaolin and bentonite), activated alumina, and carbon nanomaterials (such as carbon nanotubes and graphene) [7].

Among other adsorbent materials, graphene exhibits better adsorption capacity for Pb^{2+} removal [8]. Graphene can be represented by a honeycomb structure of a single layer of sp^2 carbon atoms packed into two-dimensional carbon nanomaterial with good thermal stability and excellent surface properties [9]. The oxidation of graphene will produce a graphene oxide (GO) that contains various types of reactive oxygen functional groups, such as hydroxyl, epoxy, carbonyl, and carboxyl groups [10]. Due to oxygen-containing functional groups in GO, a significant negative surface charge and hydrophilicity were developed. Metal oxide nanoparticles have unique characteristics that allow them to be utilised as Pb^{2+} adsorbents, such as high stability in water, well-defined pore sizes, and various functional groups on the surface [11]. The combination of GO with metal oxide nanoparticles is projected to improve the adsorption of Pb^{2+} in wastewater. Since there is a significant van der Waals interaction between the graphene layers, it is anticipated that incorporating a mixture of metal oxide nanoparticles will improve the surface properties of GO.

Iron (III) oxide (Fe_2O_3) is a stable haematite with attractive magnetic characteristics at ambient conditions. The synthesis of Fe_2O_3 nanoparticles could enhance the physical properties, contributing to the high surface-to-volume ratio, ferromagnetism, and low toxicity [12]. However, the synthesis resulted in significant volume changes and agglomerations that exhibit low adsorption performance. This problem can be solved by dispersing Fe_2O_3 nanoparticles onto another form of stable materials, such as GO, that act as an ideal matrix to improve the stability of metal oxide transition [13]. The addition of Fe_2O_3 onto GO could inhibit the aggregation of GO's structure, as well as maintain the high surface area. The modification of GO/Fe_2O_3 as a magnetic adsorbent has been reported to show good adsorption performance on Pb2+ removal, with more than 90% removal [14]. Combining the magnetic characteristics into the adsorbent's composite allows the retention of remnant magnetisation so that the material can be resuspended in the liquid medium by external magnetic field removal, as shown in Fig. 1 [15]. The adsorption capacity of Pb^{2+} was determined at 150.69 mg/g using Fe_3O_4/GO nanocomposites with an initial Pb^{2+} concentration of 380 ppm [13]. Another study found that a combination of Fe_3O_4/GO adsorbent contributes 50 mg L^{-1} adsorption

https://doi.org/10.24191/esteem.v20iSeptember.2924.g1578

capacity for Pb^{2+} removal. Thus, it is anticipated to investigate the combination of GO/Fe_2O_3 adsorbent in removing Pb^{2+}.

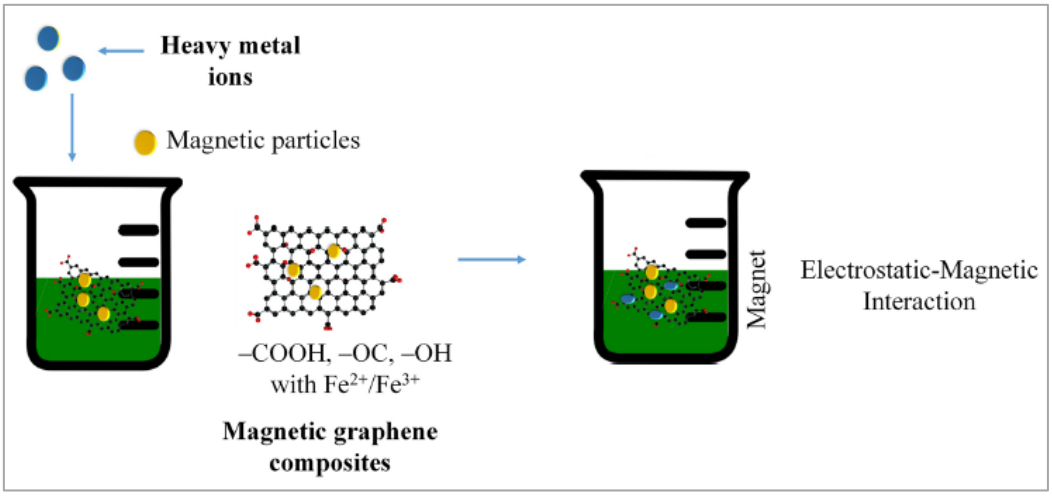

Fig. 1. Schematic diagram of removal of heavy metals using magnetic composites of GO [14].

Incorporating magnetic Fe_2O_3 nanoparticles into GO will enhance its adsorption capacity and effectiveness in adsorbing Pb^{2+} from wastewater due to its unique properties, such as a higher surface area and good surface properties. Hence, to further understand the characteristics, this work's GO/Fe_2O_3 adsorbent modification focuses on different synthesis parameters such as synthesis time, calcination temperature, and Fe_2O_3 loading weight ratio onto GO. Each parameter was analysed, and the optimum parameters that have high removal of Pb^{2+} were determined. The adsorption characteristics and kinetic study of Pb^{2+} removal using the optimised GO/Fe_2O_3 adsorbent were analysed using Langmuir and Freundlich isotherms and pseudo-first-order and second-order models, respectively.

2. METHODS

2.1 Materials and chemicals

The synthesis of GO utilising the following materials and chemicals: graphite powder (Sigma-Aldrich, 99.99%), sodium nitrate, $NaNO_3$ (Merck 99 – 100%), sulfuric acid, H_2SO_4 (Merck, 96%), potassium permanganate, $KMnO_4$ (QReC, 99%), hydrogen peroxide, H_2O_2 (R&M Chemicals, 30%), and hydrochloric acid, HCl (Merck, 37%). Then, the GO was modified using co-precipitation of iron (III) chloride hexahydrate, $FeCl_3 \cdot 6H_2O$ (Sigma-Aldrich, 97%), ammonia hydroxide, NH_4OH (R&M Chemical, 28%), ethanol, C_2H_5OH (Merck, 96%). Lead (II) nitrate $Pb(NO_3)_2$ (R&M Chemical, 99%) was used to imitate the concentration of Pb^{2+} in the wastewater. All chemicals used in this work were analytical grade.

2.2 Synthesis of graphene oxide (GO)

GO was synthesised using a Modified Hummers method [16]. Under stirring, 60 mL of H_2SO_4 was added into a beaker containing 2.5 g of graphite powder. The solution was mixed with 1.25 g of $NaNO_3$. The beaker-containing solution was kept in an ice bath and continuously stirred for 2 h at a constant temperature (0 – 6 °C). Then, 7.5 g of $KMnO_4$ was added gradually while ensuring the reaction temperature was lower than 10 °C (by controlling the amount of $KMnO_4$ added in the ice bath). The solution was continuously stirred for 2 h until the temperature reached 30°C and the colour of the solution became pasty brownish. Slowly, 135 mL of deionised (DI) water was added to the solution, then heated to 60 °C in an oil bath for 1 h before being cooled to room temperature. Next, 25 mL of H_2O_2 was added dropwise, stirring

https://doi.org/10.24191/esteem.v20iSeptember.2924.g1578

the mixture for 10 min to develop a golden yellowish colour. 50 mL HCl and 50 mL DI water were added to the solution prior to the centrifuge at 4000 rpm for 10 min to remove the remaining metal ions. The supernatant was decanted away, while the GO residuals were collected and washed with DI water until pH approaching 5 – 6. The synthesised GO was dried in an oven at 90 °C for 24 h for further use.

2.3 Synthesis of GO/Fe_2O_3 adsorbent

GO/Fe_2O_3 was synthesised using the co-precipitation method [15]. A 1 g GO powder was dispersed into 100 mL of ethanol. The mixture was sonicated for 2 h before adding 0.5 g of $FeCl_3 \cdot 6H_2O$ dissolved in 100 mL of distilled water. The sonication was continued for another 1 h at 80 °C. Then, 50 mL of 2M of NH_4OH was used as a precipitating agent, where it was gradually dropped to maintain a pH value of 11. The mixture was continuously sonicated for another 3 h at 80 °C. The precipitate was collected by centrifugation at 4000 rpm for 10 min. Next, the precipitate was washed with distilled water and ethanol several times before drying in an oven at 95 °C. Then, the calcination process proceeded at 700 °C with a heating rate of 10 °C.min^{-1} for 4 h. The GO/Fe_2O_3 adsorbent was stored in a desiccator before the Pb^{2+} adsorption experiment. Different synthesis parameters were varied, and the synthesis of GO/Fe_2O_3 was repeated by varying the synthesis time at 40, 60, 80, 120 and 140 min, calcination temperature at 400, 500, 600 and 700 °C, and GO to Fe_2O_3 weight loading at 1:0.5, 1:1, 1:1.5, 1:2.0 and 1:2.5 g. The synthesis parameters' lower limits were established based on previous research findings and following one factor at a time (OFAT) approach.

2.4 Pb^{2+} batch adsorption experiment

Batch adsorption experiments were employed using $Pb(NO_3)_2$ to simulate Pb^{2+} concentration in water [17]. A 1 L stock solution of Pb^{2+} was prepared at the desired concentration. To evaluate the effect of different synthesis parameters on Pb^{2+} removal, a stock solution of 100 mg/L was used. A 50 mL Pb^{2+} solution was placed in a beaker with 20 mg of GO/Fe_2O_3 adsorbent under constant stirring in an orbital shaker at 150 rpm for 30 min. The solution was then filtered, and the removal of Pb^{2+} was measured using inductively coupled plasma optical emission spectroscopy (ICP-OES). The Pb^{2+} removal efficiency R (%), was calculated using Eq. 1 and the amounts of Pb^{2+}adsorbed onto the GO/Fe_2O_3 adsorbent were computed using Eq. 2.

$$R\,(\%) = \left[\frac{(C_o - C_t)}{C_o}\right] \times 100\% \tag{1}$$

$$Q_e = \frac{(C_o - C_t)\,V}{m} \tag{2}$$

where C_o is the initial Pb^{2+} concentration, mg/L, C_t is the residual Pb^{2+} concentration in solution at any time t (min), mg/L, Q_e (mg/g) was the adsorption capacity at any time t (min), V (L) is the volume of the solution and m (g) is the mass of adsorbent used.

The adsorption characteristics of Pb^{2+} using the synthesised GO/Fe_2O_3 adsorbent were evaluated at different adsorption operating parameters: contact time (15, 30, 45, 60, and 75 min), adsorption temperature (35, 40, 45, 50, 55 °C), and initial Pb^{2+} concentration (50, 100, 150, 200, 250 mg/L). All experiments were triplicate and followed a one-factor-at-a-time approach.

2.5 Characterisations

The characterisation study is performed by analysing the physical properties of GO/Fe_2O_3, such as N_2 sorption-desorption and Thermogravimetric (TGA) analysis using Thermal Advantage Q Series (TA 1000). The content of each component in the prepared composite can be determined using the TGA technique through oxidative decomposition. TGA curves of pure GO composite and GO/Fe_2O_3 were performed in air

https://doi.org/10.24191/esteem.v20iSeptember.2924.g1578

at a heating rate of 10°C/min. Surface area measurements according to the Brunauer-Emmett-Teller (BET) method, along with pore size and volume analysis, were conducted by degassing at 383K for 12 h using N_2 sorption-desorption analysis (Micromeritics ASAP 2020).

2.6 Adsorption isotherms

The adsorption isotherms of Pb^{2+} removal were analysed using Langmuir and Freundlich isotherms at different concentrations of Pb^{2+}. Linear equations of the isotherms are shown in Eq. 3 and Eq. 4 [18].

$$\frac{C_e}{Q_e} = \frac{1}{Q_m} C_e + \frac{1}{K_L Q_m} \tag{3}$$

$$lnQ_e = lna_F + b_F \, lnC_e \tag{4}$$

where K_L and Q_m are the Langmuir isotherm constant related to the binding energy and monolayer adsorption capacity, a_F and b_F are the Freundlich constant in which b_F measures the surface heterogeneity.

2.7 Adsorption kinetics

To investigate the kinetics of Pb^{2+} adsorption using modified GO/Fe_2O_3, the effect of contact time on the adsorption capacity of Pb^{2+} was analysed using Pseudo first-order and second-order kinetic models, as shown in Eq. 5 and Eq. 6 [18]. Kinetic studies of Pb^{2+} removal by GO/Fe_2O_3 adsorbent were conducted at five various contact times of 15, 30, 45, 60, and 75 min at a fixed temperature of 45 °C in an incubator shaker.

$$ln(Q_e - Q_t) = -k_1 t + ln\, Q_e \tag{5}$$

$$\frac{t}{Q_t} = \frac{1}{k_2 Q_e^2} + \frac{t}{Q_e} \tag{6}$$

where Q_t is the adsorption capacity at time t, k_1 is the pseudo-first-order rate constant, and k2 is the pseudo-second-order rate constant, respectively.

3. RESULTS AND DISCUSSION

3.1 Effect of synthesis parameters of modified GO/Fe_2O_3 on Pb^{2+} removal

The effect of synthesis parameters on the modified GO/Fe_2O_3 adsorbent towards Pb^{2+} removal was evaluated at different synthesis times (40, 60, 80, 120 and 140 min), calcination temperature (400, 500, 600 and 700 °C), and GO to Fe_2O_3 weight loading (1:0.5, 1:1, 1:1.5, 1:2.0 and 1:2.5 g). The percentage removal (%R) and adsorption capacity of Pb^{2+} were determined as presented in Fig. 2 and Table 1.

Pristine GO has 23.95 mg/g of adsorption capacity and 46.41% of Pb^{2+} removal percentage. Meanwhile, it was observed that 60 min of synthesis time gives the best GO/Fe_2O_3 adsorbent performance, with 51.45% and 26.55 mg/g of %R and adsorption capacity of Pb^{2+}, respectively. As contact time increases from 80, 120 to 140 min, the adsorption capacity decreases slowly, which are 23.75, 21.30 and 11.40 mg/g, respectively, and the percentage removal. Based on the previous study, the contact time used to sonicate the Fe_3O_4 graphene composite (FGC) is 60 min [19]. The sonication process applies vibration energy to agitate particles in the sample for a better synthesis. Zengin et al. [20] reported that activated carbon

https://doi.org/10.24191/esteem.v20iSeptember.2924.g1578

synthesised via the sonication process performs better adsorption than without it. One factor affecting the synthesis time is that the bonds between GO and Fe_2O_3 nanoparticles were established during sonication. Based on the result, 40 min is not enough time for GO and Fe_2O_3 nanoparticles to interact with each other. Therefore, a duration that is too long during the sonication process also yields poor performance in the adsorption of Pb^{2+}.

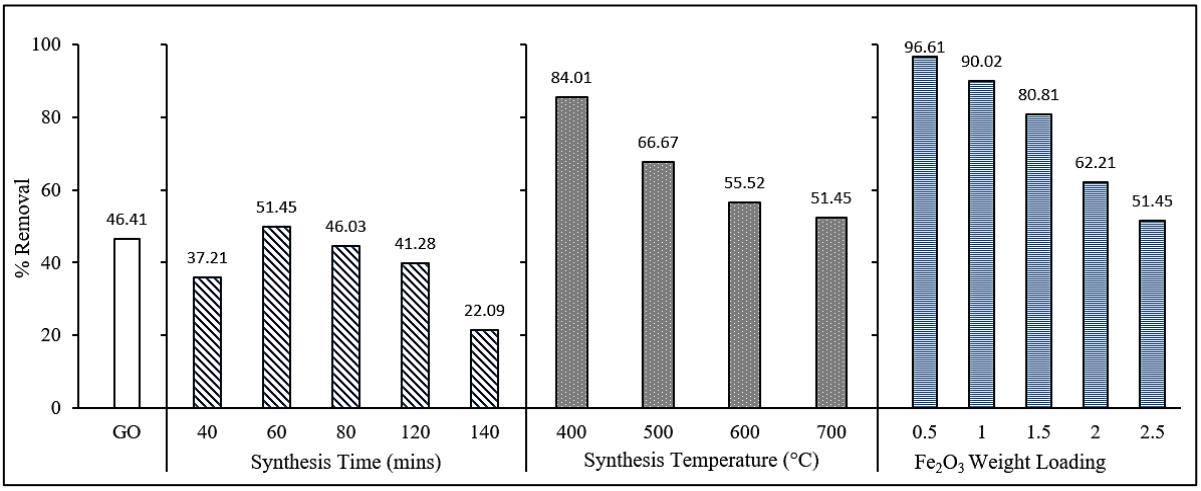

Fig. 2. % Removal of Pb^{2+} at different synthesis parameters using GO/Fe_2O_3 adsorbent.

Table 1. The adsorption capacity of Pb^{2+} at different synthesis parameters.

Parameters	Adsorption capacity, Qe (mg/g)
Synthesis time (min)	
GO	23.95
40	19.2
60	26.55
80	23.75
120	21.3
140	11.4
Synthesis temperature (°C)	
400	43.35
500	34.4
600	28.65
700	26.55
Loading weight Fe_2O_3 (g)	
0.5	49.85
1	46.45
1.5	41.7
2	32.1
2.5	26.55

The best synthesis temperature for GO/Fe_2O_3 is 400 °C, with 84.01% of Pb^{2+} removal and 43.34 mg/g of adsorption capacity. As the synthesis temperature increases from 500 to 700 °C, the adsorption capacity and percentage removal decrease slowly. Hence, the synthesis temperature at 400 °C was the best parameter

https://doi.org/10.24191/esteem.v20iSeptember.2924.g1578

to synthesise GO/Fe_2O_3. Increasing the calcination temperatures higher than 400 °C decreases the growth and formation of GO/Fe_2O_3, which reduces the surface area [21].

Ratio GO to Fe_2O_3 weight loading of 1:0.5 shows the highest %R and adsorption capacity Pb^{2+} among the others, with 96.6% and 49.85 mg/g, respectively. It has been monitored that %R of Pb^{2+} constantly drops from ratio 1:1 until ratio 1:2.5 of GO to Fe_2O_3 weight loading. The changes in the loading weight of Fe_2O_3 nanoparticles on GO are studied to see the formation of Fe_2O_3 nanoparticles onto the GO surface. The calculated results show that the higher loading of Fe2O3 nanoparticles may block the pore diameter of GO/Fe_2O_3 modified adsorbent as the Pb2+ enters the adsorbent [22]. From this work, the modified GO/Fe_2O_3 adsorbent gives the highest adsorption capacity of Pb^{2+}, which is 49.85 mg/g and has a better performance compared to graphene nanosheet adsorbent, with an adsorption capacity of Pb^{2+}, which is 22.42 mg/g. However, compared to the previous work done by Ahmad et al., the use of the ZnO/GO combination gave a higher adsorption capacity of Pb^{2+} at 418.78 mg/g [23].

3.2 Thermal stability of modified GO/Fe2O3 adsorbent

The stability of each component in the synthesised adsorbent can be determined through the TGA technique via oxidative decomposition. Fig. 3 illustrates the TGA curves of the GO samples at different GO to Fe_2O_3 weight loading ratios.

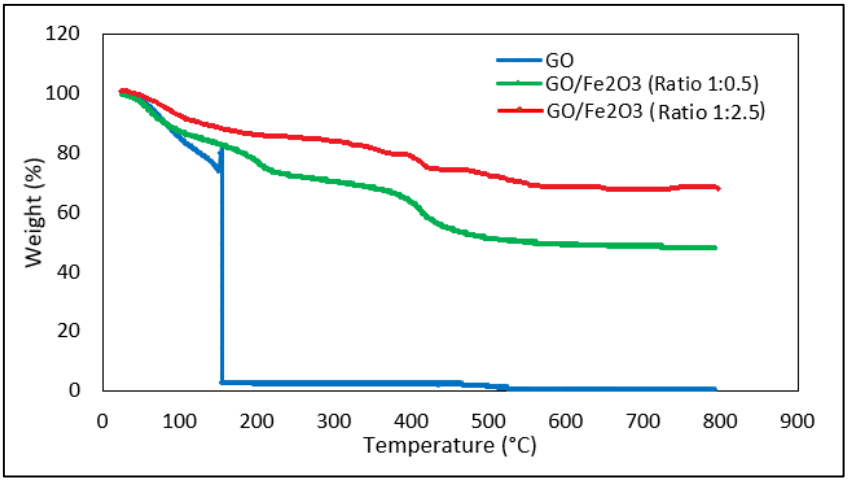

Fig. 3. Thermogravimetric analysis of GO samples at difference GO to Fe_2O_3 weight loading ratios.

The weight loss for the GO composite showed a significant difference after 150 °C; weight loss is observed at about 25%, which can be attributed to the removal of the oxygen-containing functional groups as CO, CO_2 and H_2O vapours from the sample caused by the destruction of oxygenated functional groups [24]. The most significant weight loss (74.4%) occurs in the temperature range from 150 to 530 °C. This is attributed to the thermal decomposition of some intermediate compounds containing volatile in GO. After a temperature of 530 °C, the weight of the sample tended to remain, and almost no weight loss occurred. This can be attributed to the dehydration and evaporation of fixed carbon [25].

As for GO/Fe_2O_3 adsorbent at GO to Fe_2O_3 weight loading ratio 1:0.5 and 1:2.5, the weight loss (about 17%) occurred consistently from room temperature to 100 °C, which is due to the evaporation of the physically adsorbed moisture content [24]. However, the most significant weight loss occurred for about 33% in the temperature range of 100 to 550 °C. When the temperature reached 550 °C, the weight of the sample tended to remain, and almost no weight loss occurred. According to the mass loss in the GO/Fe_2O_3 (ratio 1:0.5), about 50% of metal oxide is deposited on the surface of GO. The most significant weight loss

https://doi.org/10.24191/esteem.v20iSeptember.2924.g1578

ratio 1:2.5 is 15% in the temperature range 100 to 550 °C. According to a ratio of 1:2.5, no change in weight loss occurred after it reached a temperature of 550 °C and the weight loss of about 68% of metal oxide deposited on the surface of GO. For both ratios, as it reached the temperature of 550 °C, the weight loss remained the same, which is assumed to be the Fe_2O_3 composite left with little GO.

3.3 Adsorbent pore distribution and surface area of modified GO/Fe_2O_3 adsorbent

N_2 adsorption-desorption isotherm was used to investigate the specific surface area and pore diameter of GO/Fe_2O_3 adsorbent. Fig. 4 illustrates the adsorption-desorption isotherm for sample GO/Fe_2O_3 modified adsorbent at synthesis temperatures of 400 and 700 °C and GO to Fe_2O_3 weight loading ratio 1:0.5 and 1:2.5. The synthesised adsorbents were analysed as type-IV isotherm, indicating the mesoporous nature of materials [24]. The curve also reveals that the pore size increases between the relative pressure of 0.8 and 1.0. Fig. 5 shows the pore diameters in the 2-50 nm range, further confirming the mesoporous nature of the synthesised GO/Fe_2O_3 adsorbent [24].

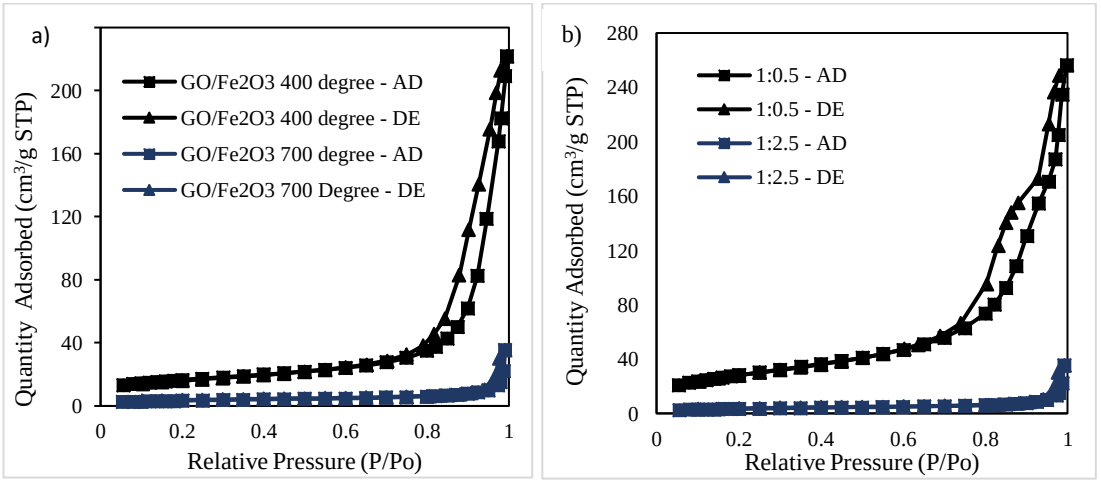

Fig. 4. N_2 adsorption-desorption isotherm of a) GO/Fe_2O_3 at 400 and 700 °C and b) GO/Fe_2O_3 at 400 °C and ratio 1:0.5 and 1:2.5.

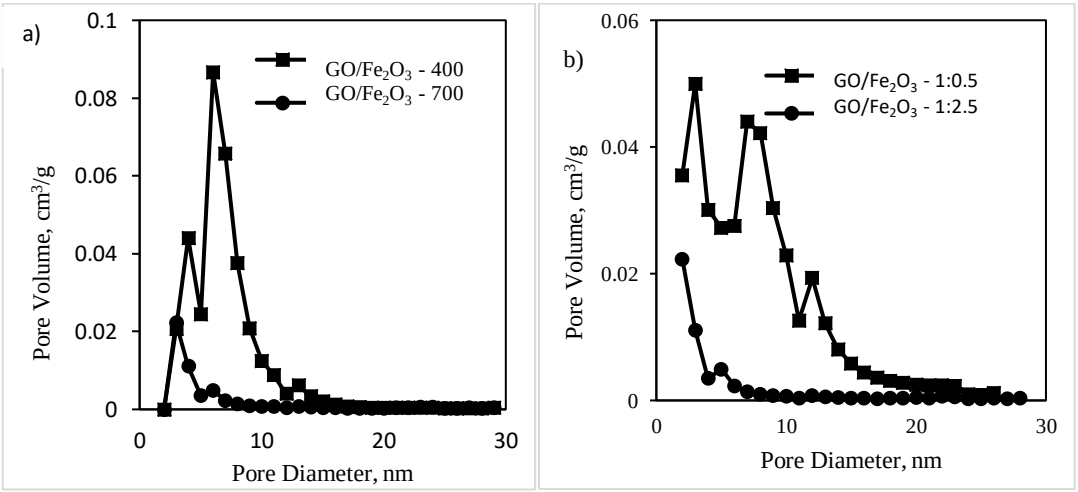

Fig. 5. Pore distribution of GO/Fe_2O_3 at a) GO/Fe_2O_3 at 400 and 700 °C and b) GO/Fe_2O_3 at 400 °C and ratio 1:0.5 and 1:2.5.

https://doi.org/10.24191/esteem.v20iSeptember.2924.g1578

Table 2 compares the pore structure between GO/Fe_2O_3 at different calcination temperatures and the GO to Fe_2O_3 weight loading ratio. According to Table 2, it is evident that the temperature calcination 400°C has a larger surface area and pore diameter, which is 55.43 m^2/g and 24.46 nm, respectively. It is confirmed that 400°C has a higher percentage of the removal than 700°C due to decreases in growth and formation of GO/Fe2O3 adsorbent as temperature increases. It is proved that the ratio 1:0.5 has a larger surface area and pore diameter, which were 98.26 m^2/g and 15.67 nm, respectively. Ratio 1:0.5 has a high surface area compared to ratio 1:2.5, which is also supported by the %R of Pb^{2+} where ratio 1:0.5 has a higher %R compared to ratio 1:2.5. This is because higher loading of Fe_2O_3 nanoparticles may block the pore diameter of GO/Fe_2O_3 modified adsorbent.

Table 2. Surface area and pore characteristics of GO/Fe_2O_3.

Adsorbent	BET surface area (m^2/g)	Pore volume (cm^3/g)	Average pore (nm)
GO/Fe_2O_3 (400°C)	55.43	0.34	24.46
GO/Fe_2O_3 (700°C)	11.54	0.06	18.59
GO/Fe_2O_3 (400°C ratio 1:0.5)	98.2	0.40	15.67
GO/Fe_2O_3 (400°C ratio 1:2.5)	11.54	0.06	18.59

3.4 Effect of adsorption parameters of Pb^{2+} removal using GO/Fe_2O_3

To evaluate the adsorption characteristics of the modified GO/Fe_2O_3 adsorbent for Pb^{2+} removal, three different adsorption parameters have been investigated, which are contact time (15, 30, 45, 60, and 75 min), adsorption temperature (35, 40, 45, 50, 55 °C), and initial Pb^{2+} concentration (50, 100, 150, 200, 250 mg/L). Fig. 6 shows the %R of Pb^{2+} at different adsorption parameters.

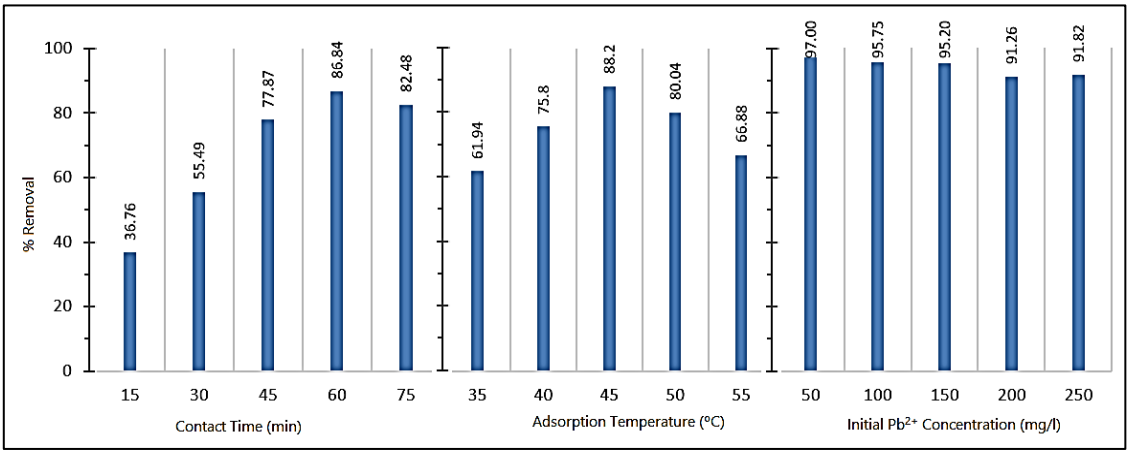

Fig. 6. Effect of contact time, adsorption temperature and initial Pb^{2+} concentration of Pb^{2+} removal using GO/Fe_2O_3 adsorbent.

From Fig. 6, as the adsorption contact time increases, the %R of Pb^{2+} increases. Once it reached 60 min, the %R of Pb^{2+} seems stagnant within 86.84 – 82.48%. This is due to the adsorption of Pb^{2+} remaining stable and steady once it reaches equilibrium within 60 min [26]. This may be justified by the fact that sufficient time is required for Pb^{2+} to achieve equilibrium. The rate of Pb^{2+} removal was higher at the initial stage due to the availability of more active sites on the surface of GO/Fe_2O_3 adsorbent, and it became slower at the later stages of contact time due to the decreased or lesser number of active sites [27]. It can be observed from Fig. 6, where the %R of Pb^{2+} increases rapidly and reaches 86.84% until 60 min of adsorption time. Beyond 60 min, the adsorption activity becomes stagnant, where little sites are left. The decrease in the %R of Pb^{2+} over time may also be due to the aggregation of Pb^{2+} around the GO/Fe_2O_3 adsorbent

https://doi.org/10.24191/esteem.v20iSeptember.2924.g1578

particles. This aggregation may hinder the migration of the Pb^{2+} adsorbate as the adsorption sites become filled up, and the resistance to diffusion of Pb^{2+} in the adsorbents increases.

Adsorption temperature contributes to a significant effect towards the %R of Pb^{2+} since the change in temperature affects the solubility of the solution and enhances the kinetic energy of the ions. Therefore, as the adsorption temperature increases to 45 ºC, the %R increases. Further than that, the %R of Pb^{2+} is decreased. This can be attributed to the fact that with the solution's temperature increase, the attractive forces between the GO/Fe_2O_3 surface and the Pb^{2+} are weakened, thus decreasing the sorption efficiency. This is due to the rise in the tendency for the Pb^{2+} to escape from the solid phase of the adsorbent to the liquid phase with an increase in temperature. When the kinetic energy of the particles is increased, the desorption rate is faster than the adsorption rate, hence decreasing adsorption efficiency. The %R of Pb^{2+} using the modified GO/Fe_2O_3 adsorbent is highest at 45 °C. That means the sorption of Pb^{2+} is in favour of temperature, which indicates that the mobility of the Pb^{2+} increases with the temperature. Therefore, it is revealed that the process is endothermic. Increasing the adsorption temperature to 55 °C shows the decrement of the %R from 88.20 to 66.88%. The increase in temperature might contribute to excess energy received by the Pb^{2+}, which resulted in less interaction with the active sites at the GO/Fe_2O_3 adsorbent surface [27].

As for the different initial concentrations of Pb^{2+}, Fig. 6 illustrates that as concentrations increase, the %R decreases. From Fig. 6, it is clearly shown that at a lower initial concentration of Pb^{2+} (50 mg/L), the amount of Pb^{2+} (adsorbate) in the solid phase of GO/Fe_2O_3 (adsorbent) was highest compared to the amount when higher concentrations were used, with 97% removal of Pb^{2+}. After 50 mg/L, no significant increase is detected in the %R of Pb^{2+}. This is because the removal of Pb^{2+} was independent of the concentration of Pb^{2+} [27].

3.5 Adsorption isotherms

To design an applicable and correct adsorption system, especially for removing heavy metal ions in wastewater, it is essential to understand the behaviour, adsorbate-adsorbent interaction, and their adsorption characteristics. Hence, a perfectly fitted isotherm model for the application is necessary [28]. Langmuir and Freundlich isotherm models were applied to evaluate the Pb^{2+} equilibrium adsorption using GO/Fe_2O_3 adsorbent in this work. The central assumption of the Langmuir isotherm model is that the development form of monolayers happens on the surface of the GO/Fe_2O_3 adsorbent. This demonstrates that just one Pb^{2+} can be adsorbed on one adsorption site, GO/Fe_2O_3 adsorbent and the intermolecular forces between them will be diminished with the distance [28]. It is likewise expected that the adsorbent surface is usually homogeneous in characteristics and possesses identical exact and energetically equivalent adsorption of Pb^{2+} from an aqueous solution [13]. In addition, the Langmuir adsorption isotherms assume that adsorption takes place at specific homogeneous sites within the adsorbent and has found successful application to many sorption processes of monolayer adsorption. While the Freundlich adsorption isotherm predicts that the enthalpy of adsorption is independent of the amount of Pb^{2+} adsorbed, the empirical Freundlich equation is based on adsorption on the heterogeneous surface. Moreover, the Freundlich equation can also be derived by assuming a logarithmic drop-off in the enthalpy of adsorption with the inclined in the fraction of occupied sites. The Freundlich equation is also purely experimentally based on Pb^{2+} adsorption on heterogeneous surfaces of GO/Fe_2O_3 adsorbent [28]. The Langmuir and Freundlich isotherm curves for Pb^{2+} removal using GO/Fe_2O_3 adsorbent are shown in Fig. 7.

Based on Fig. 7, it is observed that the Langmuir isotherm gives a better fit than the Freundlich isotherm since the correlation coefficient (R^2) values for Freundlich isotherm is higher than Freundlich isotherm (R^2 = 0.9823). Thus, Langmuir isotherm complied with the experimental data very well and proved that the monolayer adsorption of Pb^{2+} from aqueous solution onto the GO/Fe_2O_3 adsorbent with the homogeneous distribution of the Pb^{2+} adsorption of active sites on the GO/Fe_2O_3 adsorbent. Adsorption isotherm parameters were calculated and tabulated in Table 3.

https://doi.org/10.24191/esteem.v20iSeptember.2924.g1578

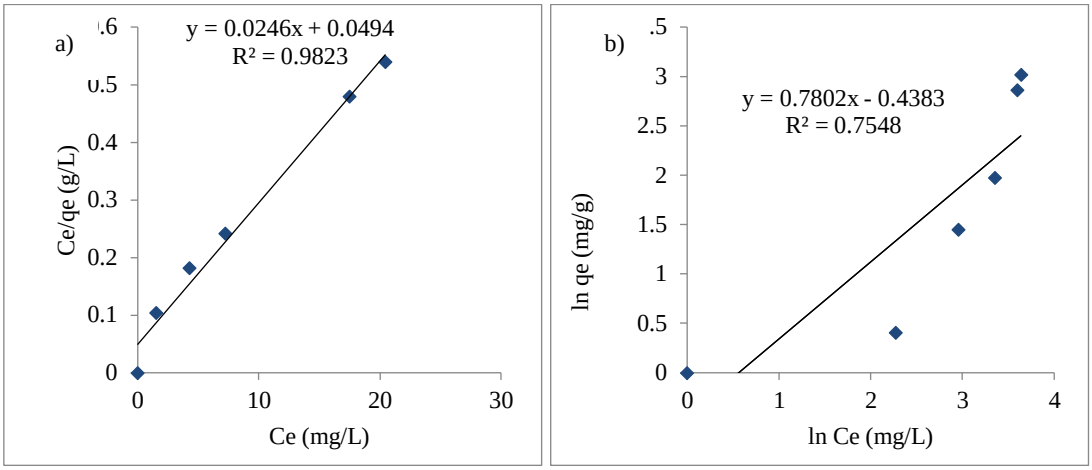

Fig. 7. Adsorption isotherms of Pb^{2+} using modified GO/Fe_2O_3 adsorbent a) Langmuir and b) Freundlich isotherms.

Table 3. Adsorption isotherms parameters for the adsorption of Pb^{2+} adsorption using GO/Fe_2O_3 adsorbent.

	Langmuir Model	**Freundlich Model**
Maximum adsorption at monolayer coverage, Q (mg/g)	40.650	-
b (L/mg)	0.4980	-
Intensity, n	-	0.7802
Freundlich constants representing the adsorption capacity, K	-	0.6451
Correlation coefficient, R^2	0.9823	0.7548

The value of b indicates the shape of the isotherms to be either unfavourable (b > 1), linear (b = 1), favourable (0 < b <1) or irreversible (b = 0). The adsorption isotherm of Pb^{2+} using GO/Fe_2O_3 adsorbent is favourable, with the value of b = 0.4980 L/mg. Thus, it confirmed the favourable removal of the Pb^{2+} from the aqueous solution in the adsorption process onto the GO/Fe_2O_3 adsorbent. The degree of favourability is generally related to the irreversibility of the system, giving a qualitative assessment of the Pb^{2+} and GO/Fe_2O_3 adsorbent interactions. The degrees tended to zero (the completely ideal irreversible case) rather than unity (representing an entirely reversible case). As for the Freundlich isotherm, the value of n (n= 0.7802) is less than 1, indicating that the adsorption process is not favourable [28]. This is also supported by the correlation coefficient value of Freundlich isotherm, R^2 = 0.7548, lower than the Langmuir isotherm value, R^2 = 0.9823. Thus, based on the comparison and criteria discussed and considered above, the equilibrium isotherm of adsorption Pb2+ from aqueous solution on GO/Fe_2O_3 adsorbent is fitted to the Langmuir isotherm model.

3.6 Adsorption kinetics

The kinetic study on the adsorption process of Pb^{2+} removal using GO/Fe_2O_3 adsorbent was analysed using two kinetics models: pseudo-first-order and second-order [29]. This is to assess the adsorption rates and to recognise the adsorption behaviour of Pb^{2+} removal on GO/Fe_2O_3 adsorbent. The adsorption kinetic of Pb^{2+} using GO/Fe_2O_3 adsorbent was plotted and shown in Fig. 8 for both pseudo-first-order and pseudo-second-order models. From the plotted kinetic models, the removal of Pb^{2+} using GO/Fe_2O_3 adsorbent best fits the pseudo-second-order model with R^2 = 0.9995. This indicates that the initial Pb^{2+} concentration plays a crucial role in determining the adsorption capacity of Pb^{2+} on GO/Fe_2O_3 adsorbent. The comparison between pseudo-first-order and second-order models for the kinetic analysis parameters of Pb^{2+} adsorption onto GO/Fe_2O_3 adsorbent is tabulated in Table 4.

https://doi.org/10.24191/esteem.v20iSeptember.2924.g1578

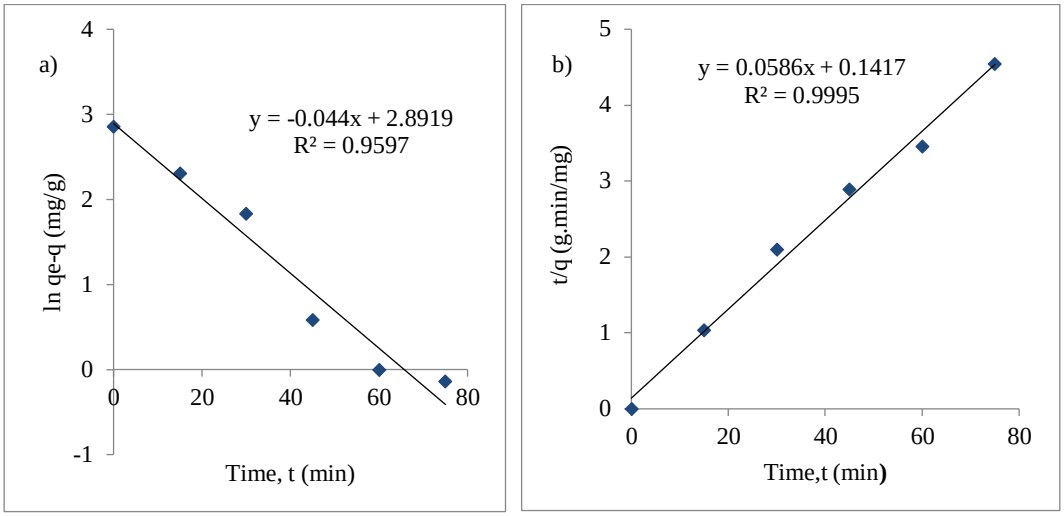

Fig. 8. Adsorption kinetics of Pb^{2+} using modified GO/Fe_2O_3 adsorbent a) Pseudo first-order and b) Pseudo second-order models.

Table 4. Kinetic analysis parameters for the adsorption of Pb^{2+} onto GO/Fe_2O_3 adsorbent.

Model	K (g/mg.min)	q (mg/g)	R^2
Pseudo first-order model	0.0440	1.5829	0.9597
Pseudo-second-order model	0.1306	7.3520	0.9995

From Table 4, it is shown that the R^2 value, 0.9995, for Pb^{2+} adsorption from aqueous solution on GO/Fe_2O_3 adsorbent in the pseudo-second-order model, is more significant than that for a pseudo-first-order model, which is only 0.9597. This indicated that it is more accurate and qualified with the pseudo-second-order model. They perfectly complied with the pseudo-second-order kinetic analysis, which determined that the adsorption mechanism relied upon the Pb^{2+} adsorbate and GO/Fe_2O_3 adsorbent. This outcome result is proven by Fick's second law of diffusion [18].

4. CONCLUSIONS

In conclusion, the synthesis of modified GO with Fe_2O_3 as an adsorbent for the removal of Pb^{2+} has been demonstrated at different synthesis parameters, which indicates that the modified GO/Fe_2O_3 has a great potential as an adsorbent for Pb^{2+} removal in wastewater. The suitable synthesis parameters of GO/Fe_2O_3 adsorbent are at synthesis temperature of 400 °C, synthesis time of 60 min, and GO to Fe_2O_3 weight loading of 1:0.5 ratio with more than 90% Pb^{2+} removal. Instead of the synthesis parameters, the adsorption operating parameters are also important. Determination of the proper operating parameters and understanding of the sorption behaviour is necessary to obtain optimum Pb^{2+} removal. The highest %R of Pb^{2+} was achieved at 97%, at 50 mg/L of Pb^{2+} initial concentration, 60 min of adsorption time, and 45 °C of adsorption temperature. The isotherms and kinetic studies indicated that the adsorption behaviour of Pb^{2+} using GO/Fe_2O_3 adsorbent is well described by the Langmuir isotherm and Pseudo second-order model.

5. ACKNOWLEDGEMENT

The authors are thankful for the monetary support and facilities Universiti Teknologi MARA Cawangan Pulau Pinang provided in completing this research work.

https://doi.org/10.24191/esteem.v20iSeptember.2924.g1578

6. CONFLICT OF INTEREST

The authors agree that this research was conducted without any self-benefits or commercial or financial conflicts and declare that there is no conflict of interest relating to the publication of this work.

7. AUTHORS' CONTRIBUTIONS

Norhusna Mohamad Nor: Conceptualisation, methodology, formal analysis, investigation and writing-original draft; **Nur Alwani Ali Bashah**: Conceptualisation, methodology, and formal analysis; **Nor Syazwani Mohamed Noor**: Conceptualisation, formal analysis, and validation; **Nur Afifah Atikha**: Conceptualisation, supervision, writing- review and editing, and validation.

8. REFERENCES

[1] T. N. B. T. Ibrahim, F. Othman, and N. Z. Mahmood, "Baseline Study of Heavy Metal Pollution in a Tropical River in a Developing Country," *Sains Malaysiana*, vol. 49, no. 4, pp. 729–742, 2020. Available: doi: 10.17576/jsm-2020-4904-02.

[2] L. Alam, "A Review on Lead (Pb) Contamination in the Drinking Water Supply at Langat River Basin, Malaysia," *MOJ Toxicol.*, vol. 3, no. 3, pp. 49–51, 2017. Available: doi: 10.15406/mojt.2017.03.00051.

[3] Department of Environment Malaysia, "Environmental Quality (Sewage and Industrial Effluents) Regulations, 1979," 1979.

[4] B. Han, C. Butterly, W. Zhang, J. Zheng He, and D. Chen, "Adsorbent materials for ammonium and ammonia removal: A review," *J. Clean. Prod.*, vol. 283, p. 124611, 2021. Available: doi: 10.1016/j.jclepro.2020.124611.

[5] B. Kamal and A. Rafey, "A mini-review of treatment methods for lead removal from wastewater," *Int. J. Environ. Anal. Chem.*, vol. 00, no. 00, pp. 1–16, 2021. Available: doi: 10.1080/03067319.2021.1934833.

[6] I. R. Chowdhury, S. Chowdhury, M. A. J. Mazumder, and A. Al-Ahmed, *Removal of lead ions (Pb2+) from water and wastewater: a review on the low-cost adsorbents*, vol. 12, no. 8. Springer International Publishing, 2022.

[7] Renu, M. Agarwal, and K. Singh, "Heavy metal removal from wastewater using various adsorbents: A review," *J. Water Reuse Desalin.*, vol. 7, no. 4, pp. 387–419, 2017. Available: doi: 10.2166/wrd.2016.104.

[8] N. R. Nik Abdul Ghani, Mohammed Saedi Jami, and K. M. Z. Ku Abdullah, "Adsorption Studies of Graphene Oxide for Lead Removal From Synthetic Wastewater," *Biol. Nat. Resour. Eng. J.*, vol. 2, no. 2 SE-Bioenvironmental Engineering, pp. 21–36, 2019.

[9] N. G. Khaligh and M. R. Johan, "Recent Advances in Water Treatment Using Graphene-based Materials," *Mini. Rev. Org. Chem.*, vol. 17, no. 1, pp. 74–90, 2019. Available: doi: 10.2174/1570193x16666190516114023.

[10] J. Wang *et al.*, "Synthesis Approaches to Magnetic Graphene Oxide and Its Application in Water Treatment: A Review," *Water. Air. Soil Pollut.*, vol. 232, no. 8, 2021. Available: doi: 10.1007/s11270-021-05281-2.

[11] B. M. Jun *et al.*, "Comprehensive evaluation on removal of lead by graphene oxide and metal organic framework," *Chemosphere*, vol. 231, pp. 82–92, 2019. Available: doi: 10.1016/j.chemosphere.2019.05.076.

[12] M. Saghi, K. Mahanpoor, and H. Shafiei, "Preparation of nano spherical α-Fe2O3 supported on 12-tungstosilicic acid using two different methods: A novel catalyst," *Iran. J. Chem. Chem. Eng.*, vol. 37, no. 1, pp. 1–10, 2018.

[13] L. T. M. Thy, P. M. Cuong, T. H. Tu, H. M. Nam, N. H. Hieu, and M. T. Phong, "Fabrication of magnetic iron oxide/graphene oxide nanocomposites for removal of lead ions from water," *Chem.*

https://doi.org/10.24191/esteem.v20iSeptember.2924.g1578

Eng. Trans., vol. 78, pp. 277–282, 2020. Available: doi: 10.3303/CET2078047.

[14] R. Kumar, S. Bhattacharya, and P. Sharma, "Novel insights into adsorption of heavy metal ions using magnetic graphene composites," *J. Environ. Chem. Eng.*, vol. 9, no. 5, p. 106212, 2021. Available: doi: 10.1016/j.jece.2021.106212.

[15] M. Jafari Eskandari and I. Hasanzadeh, "Size-controlled synthesis of Fe3O4 magnetic nanoparticles via an alternating magnetic field and ultrasonic-assisted chemical co-precipitation," *Mater. Sci. Eng. B Solid-State Mater. Adv. Technol.*, vol. 266, no. October 2020, p. 115050, 2021. Available: doi: 10.1016/j.mseb.2021.115050.

[16] M. Mukherjee *et al.*, "Ultrasonic assisted graphene oxide nanosheet for the removal of phenol containing solution," *Environ. Technol. Innov.*, Jan. 2017. Available: doi: 10.1016/J.ETI.2016.11.006.

[17] A. F. Shaaban, A. A. Khalil, B. S. Elewa, M. N. Ismail, and U. M. Eldemerdash, "A new modified exfoliated graphene oxide for removal of copper(II), lead(II) and nickel(II) ions from aqueous solutions," *Egypt. J. Chem.*, vol. 62, no. 10, pp. 1823–1849, 2019. Available: doi: 10.21608/EJCHEM.2019.11060.1713.

[18] S. Mohan, V. Kumar, D. K. Singh, and S. H. Hasan, "Effective removal of lead ions using graphene oxide-MgO nanohybrid from aqueous solution: Isotherm, kinetic and thermodynamic modeling of adsorption," *J. Environ. Chem. Eng.*, vol. 5, no. 3, pp. 2259–2273, 2017. Available: doi: 10.1016/j.jece.2017.03.031.

[19] Y. Yao, S. Miao, S. Liu, L. P. Ma, H. Sun, and S. Wang, "Synthesis, characterization, and adsorption properties of magnetic Fe 3O 4@graphene nanocomposite," *Chem. Eng. J.*, vol. 184, pp. 326–332, 2012. Available: doi: 10.1016/j.cej.2011.12.017.

[20] H. Zengin, G. Kalayci, and G. Zengin, "Effect of Sonication in the Preparation of Activated Carbon Particles on Adsorption Performance," *Sep. Sci. Technol.*, vol. 49, no. 12, pp. 1807–1816, 2014. Available: doi: 10.1080/01496395.2014.902383.

[21] L. Hou *et al.*, "Fabrication of recoverable magnetic composite material based on graphene oxide for fast removal of lead and cadmium ions from aqueous solution," *J. Chem. Technol. Biotechnol.*, vol. 96, no. 5, pp. 1345–1357, 2021. Available: doi: 10.1002/jctb.6655.

[22] H. R. Nodeh, W. A. W. Ibrahim, M. M. Sanagi, "Magnetic graphene oxide as adsorbent for the removal of lead (II) from water sample," *Jurnal Teknologi*, 78 vol. 2, pp. 25–30, 2016. Available: https://doi.org/10.11113/jt.v78.7808

[23] S. Z. N. Ahmad *et al.*, "Efficient Removal of Pb(II) from Aqueous Solution using Zinc Oxide/Graphene Oxide Composite," *IOP Conf. Ser. Mater. Sci. Eng.*, vol. 736, no. 5, 2020. Available:, doi: 10.1088/1757-899X/736/5/052002.

[24] T. Guo *et al.*, "Efficient removal of aqueous Pb(II) using partially reduced graphene oxide-Fe3O4," *Adsorpt. Sci. Technol.*, vol. 36, no. 3–4, pp. 1031–1048, 2018. Available: doi: 10.1177/0263617417744402.

[25] M. Alboghbeish, A. Larki, and S. J. Saghanezhad, "Effective removal of Pb(II) ions using piperazine-modified magnetic graphene oxide nanocomposite; optimization by response surface methodology," *Scientific Reports*, vol. 12, no. 1. 2022. Available: doi: 10.1038/s41598-022-13959-8.

[26] G. Ramezani, S. E. Moradi, and M. Emadi, "Removal of Pb^(2+) Ions from Aqueous Solutions by Modified Magnetic Graphene Oxide: Adsorption Isotherms and Kinetics Studies," *Iran. J. Energy Environ.*, vol. 11, no. 4, pp. 277–286, 2020. Available: doi: 10.5829/ijee.2020.11.04.05.

[27] X. Yang, G. Xu, and H. Yu, "Removal of lead from aqueous solutions by ferric activated sludge-based adsorbent derived from biological sludge," *Arab. J. Chem.*, vol. 12, no. 8, pp. 4142–4149, 2019. Available: doi: 10.1016/j.arabjc.2016.04.017.

[28] S. Bosu, N. Rajamohan, and M. Rajasimman, "Enhanced remediation of lead (II) and cadmium (II) ions from aqueous media using porous magnetic nanocomposites - A comprehensive review on applications and mechanism," *Environ. Res.*, vol. 213, no. March, p. 113720, 2022. Available: doi: 10.1016/j.envres.2022.113720.

[29] S. Z. N. Ahmad *et al.*, "Pb(II) removal and its adsorption from aqueous solution using zinc

https://doi.org/10.24191/esteem.v20iSeptember.2924.g1578

oxide/graphene oxide composite," *Chem. Eng. Commun.*, vol. 208, no. 5, pp. 646–660, 2021. Available: doi: 10.1080/00986445.2020.1715957.

https://doi.org/10.24191/esteem.v20iSeptember.2924.g1578